



Development of Lens Shear Panel Damper and Structural Test for Application to Building

Y. Yamasaki⁽¹⁾, M. Hada⁽²⁾, Y. Ishiwata⁽³⁾, S. Kawase⁽⁴⁾, N. Yamazaki⁽⁵⁾ and K. Kitajima⁽⁶⁾

⁽¹⁾ Research Engineer, Institute of Technology, Nishimatsu Construction Co., Ltd., yasuo_yamasaki@nishimatsu.co.jp

⁽²⁾ Research Engineer, Institute of Technology, Asunaro Aoki Construction Co., Ltd., Masaya.Hada@aaconst.co.jp

⁽³⁾ Research Engineer, Institute of Technology, Tekken Corporation, yasuihiro-ishiwata@tekken.co.jp

⁽⁴⁾ Research Engineer, Institute of Technology, Tobishima Corporation, Shouko_Kawase@tobishima.co.jp

⁽⁵⁾ Research Engineer, Institute of Technology, NIPPON CHUZO K.K., n_yamazaki@nipponchuzo.co.jp

⁽⁶⁾ Prof., Dept. of Oceanic Architecture & Eng., College of Science & Technology, Nihon Univ., kitajima.keiji@nihon-u.ac.jp

Abstract

The authors have developed a lens shear panel damper (LSPD) using low yield point steel. The LSPD is a steel damper comprising a single sheet of steel shaped like a concave lens on both sides of the center. The LSPD developed assuming lens machining added pliancy to the steel material in the center, strain to be dispersed over the entire panel and making the plate more effective in withstanding repeated deformation. The effectiveness of this lens machining has been ascertained through FEM analysis. It is proposed that the LSPD be attached to stud type. In this method, the damper (LSPD) is attached to the middle part of a stud type. Moreover, since the stud type allows the damper to be installed without obstructing openings, it is possible to improve the aseismic performance through the damping effect.

This paper describes the structural tests implemented on LSPD and also steel structure and RC structure studs fitted with LSPD. The testing on LSPD was implemented with the objective of confirming the basic performance of the dampers themselves. Adopting the type of steel and dimensions of each shape as the test parameters, force was applied based on the cycle of constant displacement and gradually increasing repetitive displacement. Results of the tests on LSPD displayed stable histories were obtained, thus confirming the energy absorption performance was excellent. When attaching the LSPD to a steel stud, the damper can be directly bound to the steel stud by means of splice plate and friction joining high-tension bolts. On the other hand, when attaching the LSPD to an RC stud, since it is necessary to do so by means of steel, two methods of attachment were devised. In the first, the LSPD was attached to a steel frame bracket, which was integrated with the RC stud by means of PC steel rod. The second proposed method was utilizing the LSPD characteristic of being a thin single sheet, this method entailed inserting the LSPD into the center of the stud. Through conducting structural tests of full-scale steel stud and RC stud fitted with LSPD, it was confirmed that the deformation of the damper was roughly equal to the deformation of the stud member. It was confirmed that LSPD performance can be adequately exhibited if the damper is attached by the proposed method.

Keywords: steel damper, low-yield-point steel, stud type, structural tests of full-scale

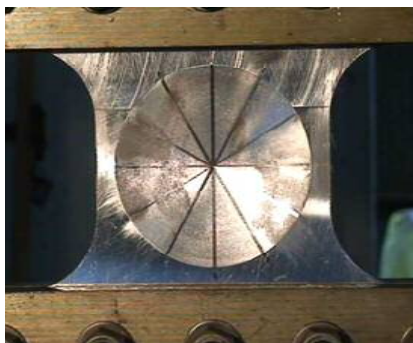


Photo 1 – Shape of the LSPD



Fig. 1 – Image of LSPD attachment



1. Introduction

In the earthquake prone nation of Japan, to control building damage caused by earthquakes, growing expectations are being placed on passively-controlled buildings that entail installing dampers in buildings [1]. In particular, more and more recently constructed buildings are adopting the passively-controlled buildings, which does not require external energy, entails a simple mechanism and is inexpensive. A variety of damping members are adopted in the passively-controlled buildings, for example, steel dampers, friction dampers, oil dampers, viscous dampers, viscoelastic dampers and so on, while various methods, such as the crossways type, shearing type, stud type, and amplifying mechanism type, are used to attach damping members.

The authors have developed a lens shear panel damper (LSPD) using low yield point steel [2] - [8]. The LSPD is a steel damper comprising a single sheet of steel shaped like a concave lens on both sides of the center. The LSPD was developed assuming attachment to studs.

2. Outline of the Lens Shear Panel Damper

Fig. 2 shows the shape of the LSPD. It is a steel damper comprising a single sheet of steel shaped like a concave lens on both sides of the center. The LSPD developed assuming lens machining added pliancy to the steel material in the center, strain to be dispersed over the entire panel and making the plate more effective in withstanding repeated deformation. Fig. 3 shows the composite members of the LSPD. The LSPD is the main damper body, while the splice plates and high-tension bolts join the main damper body with the peripheral members.

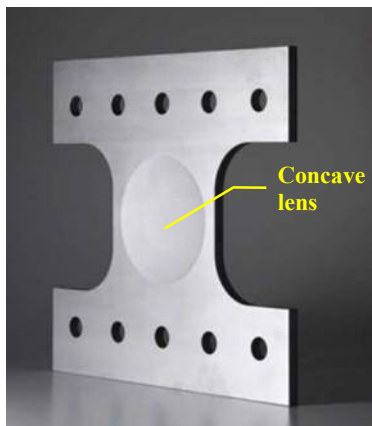


Fig. 2 – Shape of the LSPD

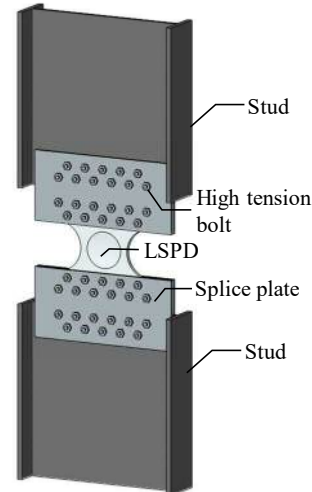


Fig. 3 – LSPD component members

Fig. 4 shows an image of LSPD attachment. The method of attaching to stud type is assumed here. This method is attaching the damper (LSPD, etc.) to the center of a stud. The advantage of this approach is that it enables dampers to be installed without obstructing openings, thereby making it possible to improve the aseismic performance through the damping effect. Low yield point steel, namely LY100 and LY225, which is endowed with expansion performance, is used as the LSPD material. The expansion performance of low yield point steel is roughly two times greater than that of general steel, and this characteristic is utilized to realize high energy absorption performance.



Since the LSPD is a steel hysteretic damper, its shear capacity is proportional to the cross-sectional area of the steel, so the scale effect is generally thought to be small. Accordingly, the mechanical characteristics of LSPD are dependent on the cross-sectional shape of the concave lens part of the shear panel. The basic shape of the LSPD is determined according to the ratio based on the plate thickness “ T ”. Fig. 5 shows the basic shape of the LSPD. It is a square shape in which the panel width and height are 13 times the plate thickness “ T ”. The central part of the panel has a concave lens for expanding the elastoplastic range. The ratio of the plate thickness at the center of the concave lens and the panel plate thickness is 1:2. Fillets are formed in the four corners of the panel to mitigate stress concentration. The LSPD plate thickness “ T ” ranges from 12mm to 24mm. Hereafter, plate that is 12mm thick overall and 6mm thick at the lens center is referred to as “Type 12-6”.

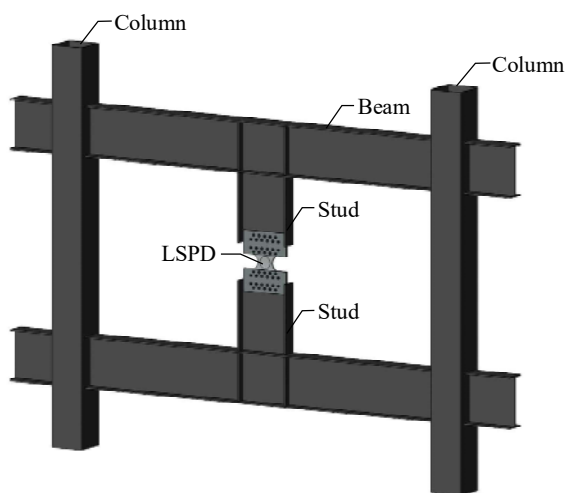
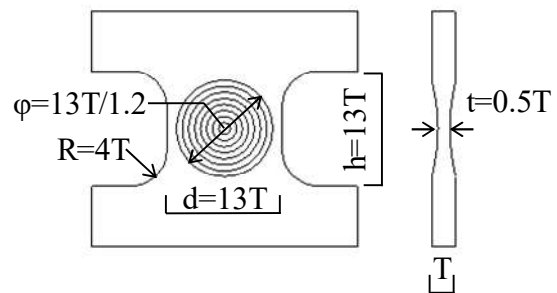


Fig. 4 – Image of LSPD attachment
(Steel structure building)



h : Effective height, d : Width, R : Fillet,

ϕ : Outer diameter of shaped concave lens

Fig. 5 – Basic shape of the LSPD

3. FEM Analysis of Lens Shear Panel Damper

3.1 Outline of the Analysis

3D FEM analysis was implemented to analytically ascertain the effectiveness of lens machining. The analysis model entailed Type 12-6 and a Type 12-6 having the same shape but without the lens machining. Solid elements were used for modeling the analysis. As material characteristics, general steel values, i.e. Young's modulus of $E=205000\text{N/mm}^2$ and Poisson's ratio of $\nu=0.3$, were adopted to impart elasticity. As boundary conditions, the upper and lower bolts were fixed in their central positions. As external force, forced displacement was imparted to the upper bolt in the horizontal direction.

3.2 Results of the Analysis

Fig. 6 shows the strain distribution derived from the FEM analysis. Fig. 6 a) shows the results for Type12-6 (with lens shape). It can be confirmed that the strain is efficiently distributed around the fillets and the central concave lens area. Fig. 6 b) shows the results for the type without the lens shape. This shows that the strain is concentrated only on the fillets. From these findings of the FEM analysis, it was confirmed that strain dispersed over the entire panel by the lens machining.

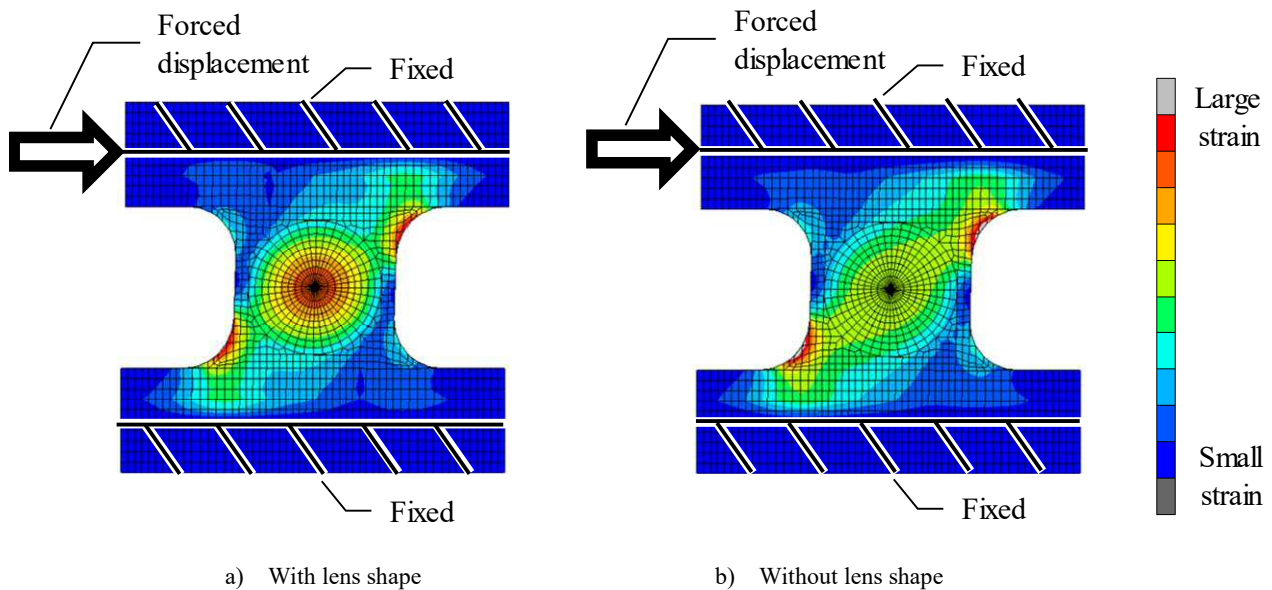


Fig. 6 – Strain distribution

4. Structural Test of Lens Shear Panel Damper

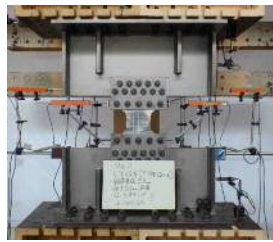
4.1 Outline of Test

Structural testing was conducted on the LSPD to confirm its basic performance. Table 1 shows the list of test specimens. As the test specimen parameters, two shapes, i.e. Type12-6 and Type24-12, and two types of steel, i.e. LY100 and LY225 were adopted. Photo 2 shows the method of attaching the LSPD. The LSPD specimens were attached to steel frame studs.

Photo 3 shows the loading device. As external force, positive and negative gradually increased and constant displacement were conducted. This was intended to confirm the basic performance of the LSPD and the performance under the design maximum displacement. For loading control, load control was adopted in the vertical direction, while the axial force was kept constant at 0kN. In the horizontal direction, load control and displacement control were adopted. As the loading cycle, initially load control was adopted to ascertain the elastic stiffness, and force of $\pm 100\text{kN}$ and $\pm 400\text{kN}$ was applied to Type12-6 and Type24-12, respectively. In the subsequent external force, gradually increasing displacement of $\pm 5\text{mm}$ or constant displacement of $\pm 35\text{mm}$ was adopted for Type12-6, while gradually increasing displacement of $\pm 10\text{mm}$ or constant displacement of $\pm 70\text{mm}$ was adopted for Type24-12. The number of cycles was set as one for the gradually increased displacement and three times for the constant displacement.

Table 1 – List of test specimen

No.	Shape	Material	Loading method	Number of cycles
1	Type12-6	LY100	$\pm 5\text{mm}$ gradual increase	1 cycle each
2	Type12-6	LY225	$\pm 5\text{mm}$ gradual increase	1 cycle each
3	Type24-12	LY225	$\pm 10\text{mm}$ gradual increase	1 cycle each
4	Type12-6	LY225	$\pm 35\text{mm}$ constant	3 cycles
5	Type24-12	LY225	$\pm 70\text{mm}$ constant	3 cycles



a) Type12-6



b) Type24-12

Photo 2 – LSPD attachment method



Photo 3 – Loading device

4.2 Test Results

Fig. 7 shows the results of the gradually increased displacement test on the Type12-6 LY100 and LY225 test specimens. Although a slight decline in load was seen at the maximum displacement of ± 35 mm, the test results displayed stable hysteresis. The horizontal load displayed a trend of increase due to the impact of strain hardening in line with the gradually increased displacement. It was confirmed that even if out-of-plane deformation arises in the LSPD, it does not accompany a sudden decrease in load.

Fig. 8 shows the relationship between the average shearing stress and strain in the Type12-6 and Type24-12 test specimens made of LY225. Here, the average shearing stress was obtained through dividing load by the cross-sectional area, while strain was sought through dividing deformation by width. Fig. 8 a) and b) show the test results for positive and negative gradually increased displacement and constant displacement, respectively. From Fig. 8 a), since Type12-6 and Type24-12 generally display similar stable hysteresis, it can be confirmed that the scale effect is small. Moreover, from Fig. 8 b), it can be confirmed that stable hysteresis is also derived at constant displacement.

From the results of testing on LSPD specimens, stable histories were obtained, thus confirming the energy absorption performance was excellent. Also, it was confirmed that the scale effect of LSPD is small.

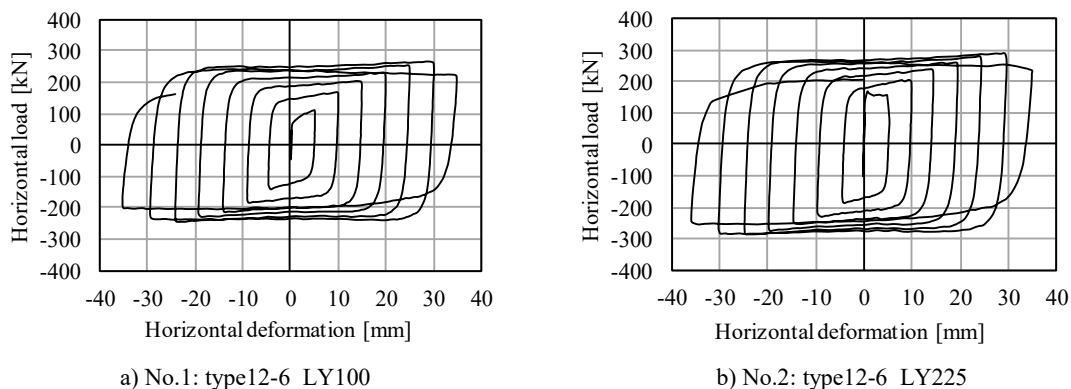


Fig. 7 – Horizontal load - horizontal deformation relationship

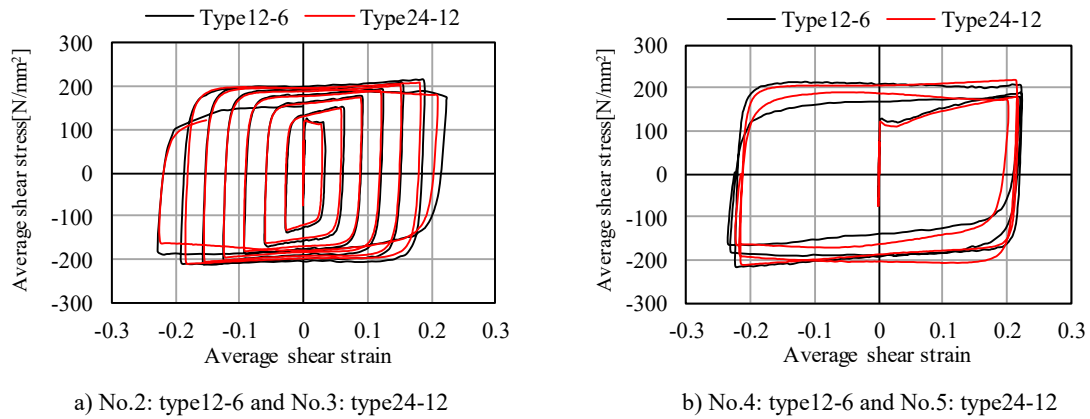


Fig. 8 – Average shear stress - average shear strain relationship

5. Structural Test of Steel Structure Stud Fitted with Lens Shear Panel Damper

5.1 Outline of Test

It is proposed that the LSPD be attached to a stud. This chapter describes structural test assuming the LSPD is attached to a steel structure stud.

Fig. 9 shows the test specimen. The steel frame stud measured BH-600 x 250 x 16 x 32 and was made of SN490. The LSPD shape was Type12-6 and material was LY225. Photo 4 shows the loading device. Load control was adopted in the vertical direction, while the axial force was kept constant at 0kN. In the horizontal direction, displacement control was adopted with positive and negative gradually increased displacement. The loading cycle is indicated in Fig. 10.

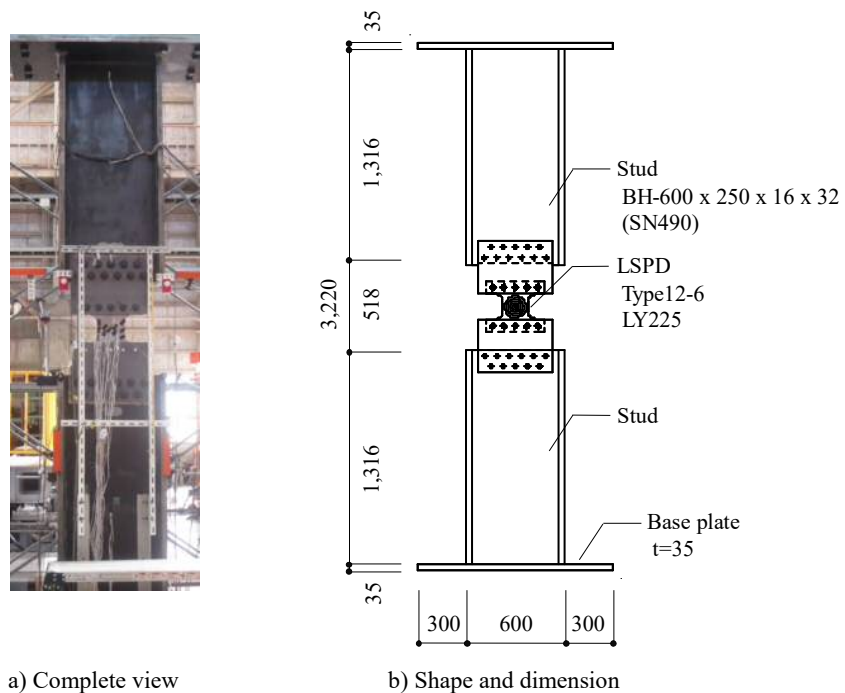


Fig. 9 – Steel structure stud test specimen



Photo 4 – Steel structure stud loading device

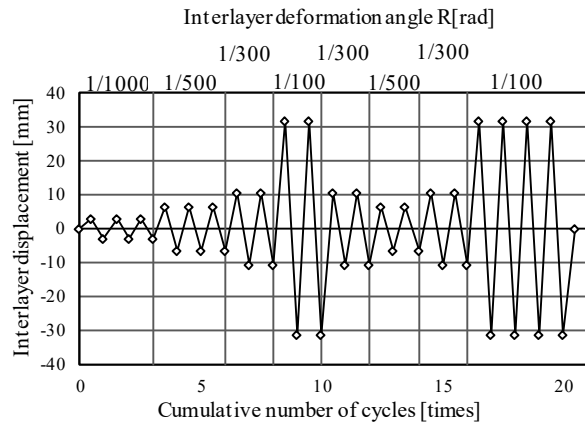


Fig. 10 – Steel structure stud loading cycle

5.2 Test Results

As a result of the tests, Fig. 11 shows the horizontal load - interlayer deformation relationship. The LSPD test specimen experienced shear yielding in the first cycle at the interlayer deformation angle of 1/540rad. The horizontal load at that time was 156kN. The horizontal load displayed a trend of increase due to the impact of strain hardening in line with the gradually increased displacement and the repeated displacement. The maximum horizontal load of -285kN occurred in the ninth cycle (test specimen interlayer deformation angle: $R=1/100$ rad). Moreover, although out-of-plane deformation started to occur in the 17th cycle ($R=1/100$ rad), no decline in horizontal load was observed and the horizontal load reached -284kN in the 18th cycle. Thus, even if out-of-plane deformation does arise in the LSPD, it does not entail sudden decline in load.

Accordingly, it was confirmed that the LSPD performance can be adequately exhibited if the proposed method of attachment to steel stud is adopted.

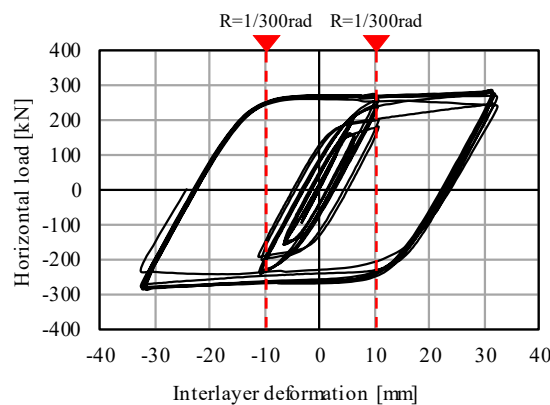


Fig. 11 – Horizontal load - interlayer deformation relationship



6. Structural Test of RC Structure Stud Fitted with Lens Shear Panel Damper

6.1 Outline of Test

This chapter describes structural test assuming that the LSPD is attached to an RC stud. When attaching the LSPD to an RC stud, since it is necessary to do so by means of steel, two methods of attachment were devised. Two test specimens were used: the RCT test specimen using PC steel rods, and the RCA test specimen embedded in the stud. The following sections describe the common matters and the respective features of each type at the time of planning.

6.1.1 Common Matters in Test Specimen

As common matters regarding the test specimens, assuming installation to communal housing on the balcony side, the RC stud cross section was set as 250mm x 1100mm, the concrete design standard strength was $F_c = 33\text{N/mm}^2$, and the LSPD was Type12-6 made from LY225 steel. The test section was set between an upper and lower stud with inner height (stud height) of 2000mm.

6.1.2 RCT Test Specimen

Fig. 12 shows the RCT test specimen. The RCT test specimen was attached to the upper and lower studs by means of a steel frame bracket (SS400) using two PC steel rods on each end. The LSPD was attached to the steel frame bracket by friction joining high-tension bolts. Axial load of 457kN (tension when fixed) was imparted to each PC steel rod, and the test specimen was made not cracking of the RC stud with respect to the LSPD's design maximum horizontal load (340 kN). 4-D19 (SD345) was used as the main reinforcement of the RC stud.

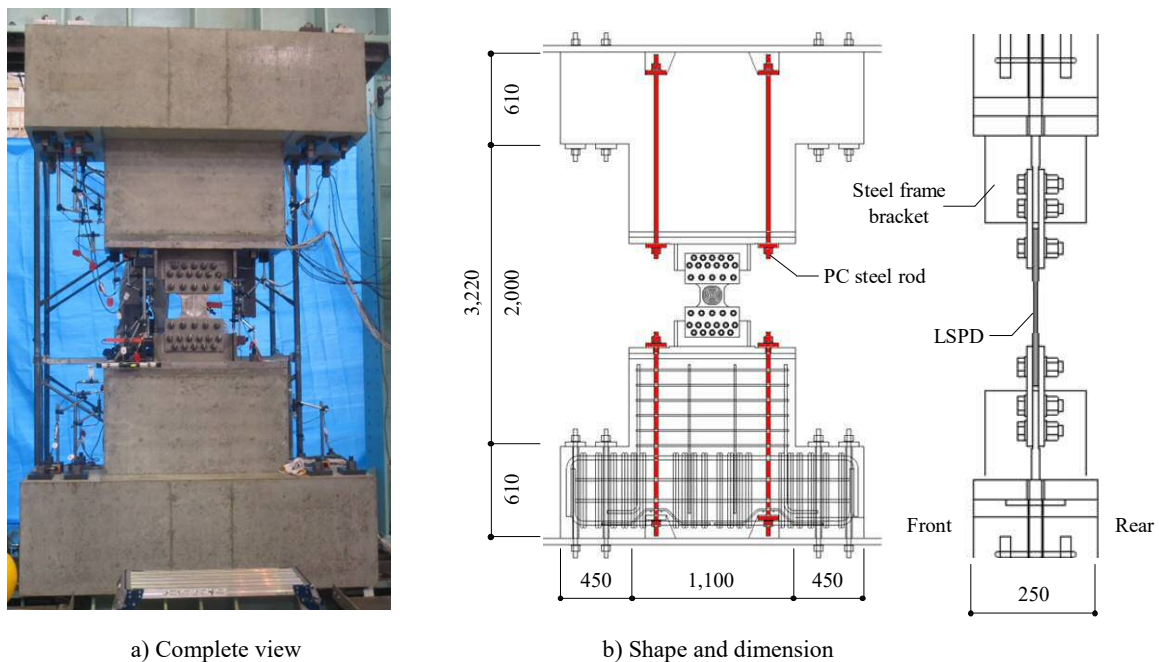


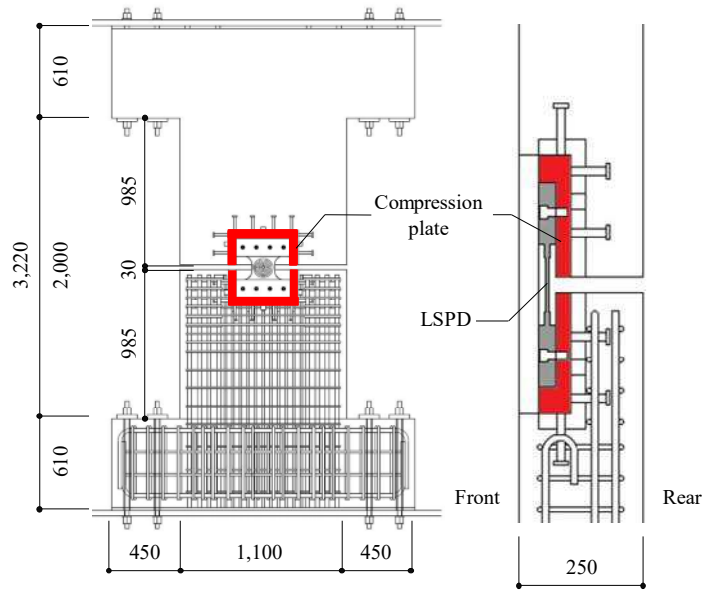
Fig. 12 – RCT test specimen

6.1.3 RCA Test Specimen

Fig. 13 shows the RCA test specimen. The RCA test specimen was made by fitting the LSPD into a compression plate (SS400) embedded in the RC stud and attaching it by using hexagonal bolts. The compression plate was fixed by means of headed studs and shear key. Cracking of the RC stud with respect to the LSPD's design maximum horizontal load was allowed, however, the test specimen made use of the LSPD feature of a thin single sheet. 20-D25(SD345) was used as the main reinforcement of the RC stud.



a) Complete view



b) Shape and dimension

Fig. 13 – RCA test specimen

6.2 Outline of Loading Plan

Photo 5 shows the loading device. Load control was adopted in the vertical direction, while the axial force was kept constant at 0kN. In the horizontal direction, displacement control was adopted with positive and negative gradually increased displacement. The loading cycle is indicated in Fig. 14. Loading was most commonly applied on the test specimen at interlayer deformation angle of 1/200rad with a view to ascertaining performance in the case where small and medium earthquakes repeatedly occur.

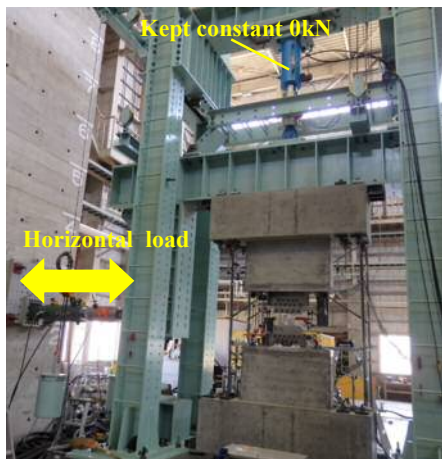


Photo 5 – RC structure stud loading device

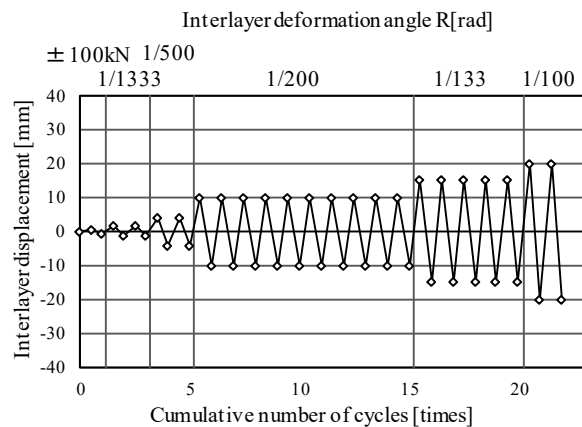


Fig. 14 – RC structure stud loading cycle

6.3 Test Results

6.3.1 RCT Test Specimen

As a result of the tests, Fig. 15 shows the horizontal load - interlayer deformation relationship and cracking over the entire RCT stud. The RCT experienced shear yielding in the second cycle when the horizontal load



on the positive side ($R=1/1333$ rad) was 147 kN. From the interlayer deformation angle of $1/500$ rad and beyond, the horizontal load displayed a trend of increase due to the impact of strain hardening in line with the gradual increase of displacement. A stable hysteresis loop was derived at the interlayer deformation angles of $1/200$ and $1/133$ rad. The maximum horizontal load of -266 kN occurred in the 17th cycle on the negative side ($R=1/133$ rad). Out-of-plane deformation started to occur in the LSPD in the 20th cycle on the negative side ($R=1/133$ rad), however, no decline in horizontal load was observed. Cracking started to occur on the lower right fillet of the LSPD in the 21st cycle on the negative side ($R=1/100$ rad) and the horizontal load gradually started falling from here, although the shape of the hysteresis loop was maintained.

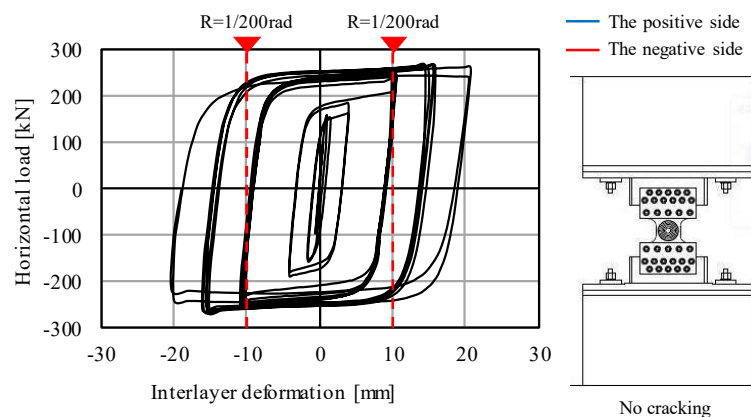


Fig. 15 – RCT load - deformation relationship and Cracking diagram

6.3.2 RCA Test Specimen

As a result of the tests, Fig. 16 the horizontal load - interlayer deformation relationship and cracking over the entire RCA stud. The RCA experienced shear yielding in the 2nd cycle when the horizontal load on the positive side ($R=1/1333$ rad) was 132kN. Cracking was visually confirmed in the corner of the lower stud edge and compression plate in the 2nd cycle (at the time of LSPD yielding). Shear cracking was confirmed on the lower stud in the 9th cycle on the positive side ($R=1/200$ rad) and the 18th cycle on the negative side ($R=1/133$ rad), and on the upper stud in the 16th cycle on the positive side ($R=1/133$ rad), although a stable hysteresis loop was derived. Out-of-plane deformation started to occur in the LSPD in the 20th cycle on the negative side ($R=1/133$ rad), however, no decline in horizontal load was observed. The maximum horizontal load of -266 kN occurred and cracking occurred on the LSPD top left fillet in the 22nd cycle on the negative side ($R=1/100$ rad).

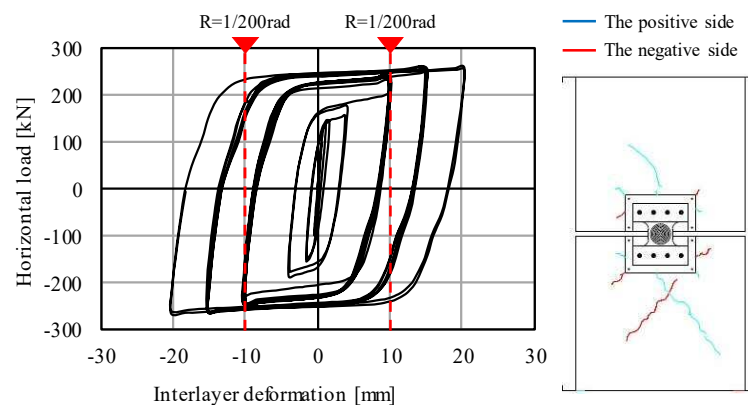


Fig. 16 – RCA load - deformation relationship and Cracking Diagram



6.3.3 Changes in the Deformation Ratio

Fig. 17 shows changes in the ratio of LSPD deformation component out of the overall stud deformation (interlayer deformation). Here, the ratio was calculated by dividing the incremental amount of LSPD deformation in each cycle from 0kN load to peak load by the incremental amount of interlayer deformation.

Looking at the ratio of LSPD deformation in the RCT and RCA test specimens, the LSPD deformation component accounted for approximately 40% of the overall deformation at the ± 100 kN positive and negative peaks. After the LSPD yielded, the ratio of the LSPD deformation component increased, becoming approximately 90% at $R=1/200$ rad and beyond. A similar trend was displayed in each cycle for both methods of attachment. Concerning the RCA, cracking occurred on the stud throughout the overall experiment, however, the LSPD deformation component sustained a high ratio.

Accordingly, it was confirmed that LSPD performance can be adequately exhibited if the LSPD is attached to an RC stud using the proposed method.

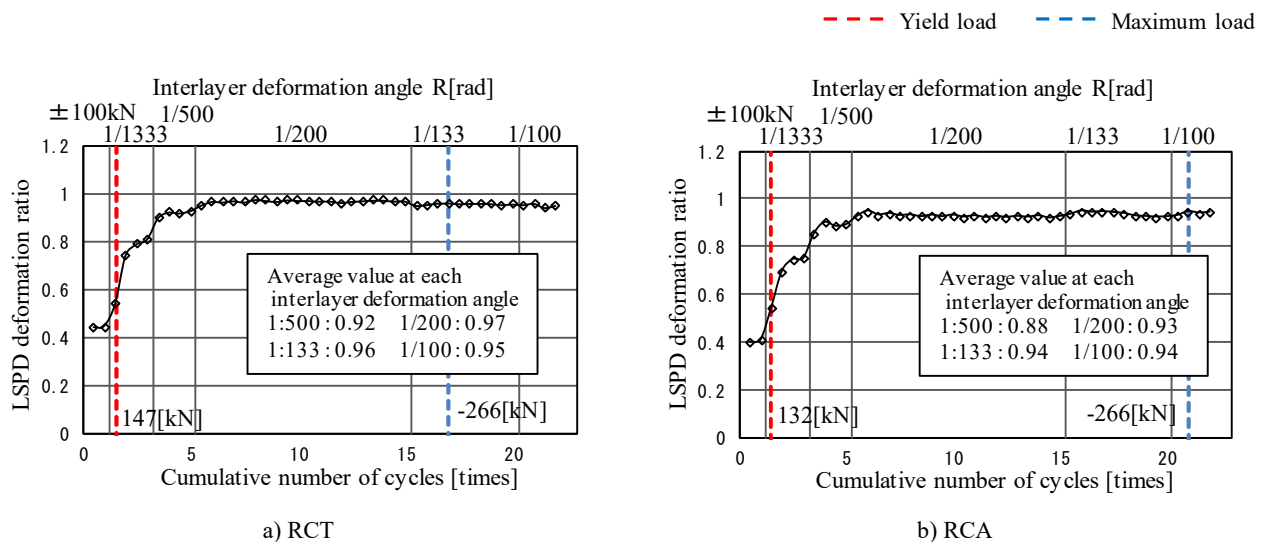


Fig. 17 – LSPD deformation ratio

7. Summary

This paper described structural tests implemented on LSPD and also steel structure and RC structure studs fitted with LSPD.

- 1) In Chapter 2, an outline description of the LSPD was given. The LSPD is a steel damper comprising a single sheet of steel shaped like a concave lens on both sides of the center. The LSPD developed assuming lens machining added pliancy to the steel material in the center, strain to be dispersed over the entire panel and making the plate more effective in withstanding repeated deformation.
- 2) In Chapter 3, the 3D_FEM analysis that was implemented to analytically ascertain the effectiveness of lens machining was described. From the findings of the FEM analysis, it was confirmed that strain dispersed over the entire panel by the lens machining.
- 3) In Chapter 4, structural test implemented on LSPD was described. From the results of testing on LSPD specimens, stable histories were obtained, thus confirming the energy absorption performance was excellent. Also, it was confirmed that the scale effect of LSPD is small.
- 4) In Chapter 5 and Chapter 6, structural test implemented on full-size steel and RC studs fitted with LSPD was described. Through the testing, it was confirmed that the deformation of the damper was roughly equal to the deformation of the stud member. The RCA, cracking occurred on the stud throughout the



overall experiment, however, the LSPD deformation component sustained a high ratio. Accordingly, it was confirmed that LSPD performance can be adequately exhibited if the LSPD is attached to stud using the proposed method. And, it is thought that the LSPD's performance can be fully exhibited even when applied in a column-beam frame.

8. Acknowledgements

This research represents part of the work implemented by the Lens Shear Panel Damper Renovation Council (Nippon Chuzo, Tobishima Corporation, Tekken Corporation, Asunaro Aoki Construction Co., Ltd. and Nishimatsu Construction Co., Ltd.). We take this opportunity to express our gratitude to all those concerned.

9. References

- [1] The Japan Society of Seismic Isolation (2013): Manual for Design and Construction of Passively-Controlled Buildings (3rd Edition), Daioh, November 2013. (in Japanese)
- [2] Syouichi N, et.al., (2013): Study on the Shear Panel Damper in the Shape of Concave Type Lens for Seismic Response Control Structure (Part1~4). Summaries of Technical Papers of annual Meeting Architectural Institute of Japan, pp.835-842, August 2013. (in Japanese)
- [3] Nobuhiro Y, et.al., (2014): Study on the Shear Panel Damper in the Shape of Concave Type Lens for Seismic Response Control Structure (Part5~11). Summaries of Technical Papers of annual Meeting Architectural Institute of Japan, pp.851-864, September 2014. (in Japanese)
- [4] Nobuhiro Y, et.al., (2016): Experimental study of the Stud-type shear panel damper (Part1~2). Summaries of Technical Papers of annual Meeting Architectural Institute of Japan, pp.115-118, August 2016. (in Japanese)
- [5] Daiki K, et.al., (2017): Experimental Study on Structural Performance of RC Studs with Lens Damper (Part1~2). Summaries of Technical Papers of annual Meeting Architectural Institute of Japan, pp.575-578, August 2017. (in Japanese)
- [6] Yasuo Y, et.al., (2018): Study on Structural Performance of RC Studs with Lens Shear Panel Damper. Proceedings of the Japan Concrete Institute Vol.40, pp.937-942, July 2018. (in Japanese)
- [7] Takumi S, et.al., (2018): Experimental Study on Structural Performance of RC Studs with Lens Damper (Part3~4). Summaries of Technical Papers of annual Meeting Architectural Institute of Japan, pp.265-268, September 2018. (in Japanese)
- [8] Takumi S, et.al., (2019): Study on the Shear Panel Damper in the Shape of Concave Type Lens for Seismic Response Control Structure (Part12~13). Summaries of Technical Papers of annual Meeting Architectural Institute of Japan, pp.763-766, September 2019. (in Japanese)